http://dx.doi.org/10.5012/bkcs.2011.32.12.4382

The Application of TiO_2 Hollow Spheres on Dye-sensitized Solar Cells

H. J. Cho and D. Jung

Department of Chemistry and Institute of Basic Natural Sciences, Wonkwang University, Iksan, Jeonbuk 570-749, Korea
**E-mail: djung@wku.ac.kr*
Received August 3, 2011, Accepted October 22, 2011

TiO_2 hollow spheres were fabricated by using SiO_2 as an inorganic template. Spherical SiO_2 particles were coated by TiO_2 through the nucleation process, and then the core SiO_2 part was eliminated by using HF solution. Finally, TiO_2 hollow spheres were obtained. The size of the TiO_2 hollow spheres was about 300-400 nm and the thickness of the hollow wall was about 20-30 nm. The hollow has several holes whose diameters were within 100-200 nm. Dye-sensitized solar cells fabricated by using the TiO_2 hollow spheres were characterized. The solar conversion efficiency of the cell was 8.45% when TiO_2 hollow spheres were used as a scattering material, while it was 4.59% when TiO_2 hollow spheres were used as a normal electrode material.

Key Words : Template method, Hollow TiO_2, Electronic materials, Dye-sensitized solar cells

Introduction

In recent years, the field of solar energy conversion to electricity and its storage has become one of the most interesting research fields. Among the different form of photovoltaic cells, the dye-sensitized solar cells (DSSCs) have attracted considerable attention over the past decade since they offer the possibility of low cost production of photovoltaic devices alternative to the conventional silicon-based junction devices[1-4] and also provide the opportunity to produce the transparent flexible devices. Typically, the electron collecting layer in these systems is a 10 nm thick nanocrystalline film comprising of three-dimensional network of interconnected semiconducting particles sintered onto a conductive glass substrate. As opposed to silicon-based devices where the semiconductor absorbs the light and transport the released charge carriers, the two tasks are separated in a DSSC system. Upon illumination, the dye molecules are excited and initial charge separation occurs by injection of an electron from the dye into the conduction band of the semiconductor resulting in charge separation. The oxidized dye is quickly reduced by the redox electrolyte before it can recapture the injected electron. Meanwhile, the injected electron is transported in the conduction band of the semiconductor by diffusion[5] to the charge collecting conductive glass substrate from where it performs useful work in an external circuit before returning to the cell through the counter electrode to reduce the electrolyte.

For preparing high efficiency DSSCs, a high surface area of the nanostructured TiO_2 layer is essential, because it allows adsorption of sufficiently large number of dye molecules needed for efficient light harvesting. Extensive research has been conducted on TiO_2 materials with various structures, such as nanowire,[6] nanorod,[7] and nanotube.[8-10] Besides the high surface area of the TiO_2 layer, good connections between TiO_2 grains as well as a good adhesion to transparent conducting oxide (TCO) are required to diminish the reactions of photogenerated electrons with electrolyte material and to assure good electrical conductivity. Therefore, the optimization of the morphology of TiO_2 is a prerequisite for the realization of high efficiency DSSCs.[11,12] The conventional DSSC is made from nanoporous TiO_2 photoelectrode with organo-ruthenium dye as a light harvesting component. The second generation of DSSCs adopts double electrode system consisting of a semiconducting layer which is made of TiO_2 particles having about 15-20 nm-sized diameter and a light scattering layer which is made of TiO_2 particles having about 400 nm-sized diameter.[13-17] The purpose of using larger size TiO_2 particles is to increase the conversion efficiency by absorbing scattered light. The morphology of TiO_2 can be widely tuned to achieve the best efficiency. Grätzel *et al.* introduced mesoporous TiO_2 particular films as semiconducting photoanodes to enhance the effective surface area so as to absorb more dye molecules and thus more light absorption which leads to better efficiency. The photoelectrodes are commonly the three-dimensional networking of interconnected TiO_2 nanoparticles, the band gap of which matches well with the sensitized dyes. TiO_2 photoanodes are also easily prepared through environmental design at low cost.

The TiO_2 hollow spheres were synthesized by using SiO_2 as a template. The obtained hollow powders were applied for preparing DSSCs to see if they could absorb more dye molecules using their empty spaces. In this paper, the preparation of TiO_2 hollow spheres and their applications on DSSCs are investigated.

Experimental

Preparation and Characterization of TiO_2 Hollow Spheres. An appropriate amount of $TiCl_4$ was added slowly into the flask which was filled with distilled water, under magnetic stirring. The temperature of the solution was kept under 5 ^oC by using an ice-bath. After adding $TiCl_4$

thoroughly, the flask was left with continuous stirring for 1 hour to produce $TiOCl_2$ mother solution. 5 g of purchased SiO_2 particles whose diameters ranged from 200 to 400 nm were dispersed into water in a 300 mL vial, and after 150 mL of already made $TiOCl_2$ mother solution was added into the vial. The capped vial was kept at 80 °C for 2 hours under magnetic stirring to obtain TiO_2-coated SiO_2 particles. The final white precipitate was filtered and washed with de-ionized water several times. The dried particles were dispersed into already prepared 4.8% HF solution under vigorous stirring for 1 hour to eliminate SiO_2 so that TiO_2 hollow spheres were prepared. After the reaction, the sediment was filtered, washed and dried. The sample obtained after the treating with HF solution was annealed at 500 °C for 2 hours.

The crystal structures and morphologies of the products were characterized with an X-ray diffractometer (XRD) and a scanning electron microscopy (SEM), before and after the treatment with HF solution. The amount of residual SiO_2 inside the TiO_2 hollow spheres was investigated by analyzing with an X-ray fluorescence spectrometer (XRF, Bruker S4-Pioneer), also before and after the treatment with HF solution.

Preparation of Solar Cell with TiO_2 Hollow Spheres. Since the size of the prepared TiO_2 hollow spheres is about 300-400 nm, this sample was tested for two different applications; it was used as a scattering material (type B) and was used as an electrode material (type C and type D). When it was used as an electrode material, also two different types of cells were prepared; the first cell type was prepared by using TiO_2 hollow spheres as an electrode material without any scattering layer (type D) and the other cell type was with a scattering layer which was made of 400 nm sized spherical anatase TiO_2 (type C). When the sample was used as a scattering material, the electrode layer was constructed by using 13 nm sized anatase TiO_2 particles. For comparison, the standard cell which was made of 13 nm anatase TiO_2 film as an electrode layer and 400 nm sized anatase TiO_2 film as a scattering layer (type A), was also fabricated. Before preparing each layer, fluorine-doped tin oxide (FTO) glass plates (Pilkington TEC Glass-TEC 8, Solar 2.3 mm thickness) were cleaned in a detergent solution using an ultrasonic bath for 30 min and then rinsed with water and ethanol. A transparent nanocrystalline electrode layer was prepared on the FTO glass plates by using a doctor blade printing of 13 nm sized TiO_2 (type A: Solaronix, Ti-Nanoxide T/SP) or hollow TiO_2 paste (type C: with a scattering layer; type D: without a scattering layer), which was then dried for 2 h at 25 °C. The TiO_2 electrodes were gradually heated under an air flow at 325 °C for 5 min, at 375 °C for 5 min, at 450 °C for 15 min, and finally at 500 °C for 15 min. The gradual temperature raising is needed to evaporate the organic solvents step by step so that the coated TiO_2 layer does not make any crack. The thickness of the transparent layer was measured by using an Alpha-step 250 surface profilometer (Tencor Instruments, San Jose, CA). The paste containing 400 nm sized anatase particles (type A, C: CCIC, PST-400C) and the paste made of hollow TiO_2 particles (type B, C) as scattering layers were deposited by means of doctor blade printing, and then dried for 2 h at 25 °C. The TiO_2 scattering layers were also gradually heated under an air flow at 325 °C for 5 min, at 375 °C for 5 min, at 450 °C for 15 min, and at 500 °C for 15 min, respectively. The TiO_2 electrodes were immersed again in $TiCl_4$ aqueous solution at 70 °C for 30 min and sintered at 500 °C for 30 min. Then, they were immersed in N719[18,19] dye solution (0.3 mM in Ethanol, EtOH) and kept at room temperature for 24 h. Spherical TiO_2 (25 nm size) and hollow TiO_2 samples were immersed in dye solution (0.3 mM in Ethanol) for same time, and then each sample was filtered and dried. Dye absorbed in each sample was desorbed by dispersing the powders in ethanol with magnetic stirring. Two ethanol solutions were investigated by using a UV spectroscopy (Shimadzu UV 2450). Finally, the amount of dye absorbed in each sample was quantitatively examined by analyzing the peak area. FTO plates for the counter electrodes were cleaned in an ultrasonic bath in H_2O, acetone, and 0.1 m aqueous HCl, subsequently. The counter electrodes were prepared by placing a drop of H_2PtCl_6 solution (2 mg Pt in 1 mL ethanol) on an FTO plate and heating it (at 400 °C) for 15 min. The dye-adsorbed TiO_2 electrodes and the Pt counter electrodes were assembled into a sealed sandwich-type cell by heating at 80 °C using a hot-melt ionomer film (Surlyn) as a spacer between electrodes. A drop of the electrolyte solution was placed in the drilled hole of the counter electrode and was driven into the cell via vacuum backfilling. Finally, the hole was sealed using additional Surlyn and a cover glass (0.1 mm thickness). The electrolyte was then introduced into the cell, which was composed of 0.6 M 3-hexyl-1,2-dimethyl imidazolium iodide, 0.05 M I_2, 0.1 M LiI and 0.5 M *tert*-butylpyridine in acetonitrile. The photocurrent-voltage (*I-V*) curves were measured using a source measure unit under irradiation of white light from a 1,000 W Xenon lamp (class AAA K3000 solar cell I-V measurement system). The incident light intensity and the active cell area were 100 mW/cm^2 and 1.0 cm^2, respectively. The I-V curves were used to calculate the short-circuit current (I_{sc}), open-circuit voltage (V_{oc}), and overall conversion efficiency (η_{eff}) of DSSCs. The standard spectral coincidence of this equipment was AM 1.5G. The solar simulator was calibrated by using the KG5 filtered Si reference solar cell.

Results and Discussion

Structure and Shape of the Particle. The XRD patterns of TiO_2-coated SiO_2 particles and TiO_2 hollow spheres after the elimination of SiO_2 are shown in Figure 1(a) and 1(b), respectively. Anatase-type TiO_2 and SiO_2 peaks are clearly shown in TiO_2-coated SiO_2 particles (see Fig. 1(a)). Sharp peaks positioned at typical 2θ of anatase and SiO_2 represent the TiO_2-coated SiO_2 powders are successfully synthesized and crystallized. Although SiO_2 is surrounded by TiO_2, the typical SiO_2 peak at $2\theta = 27^o$ is sharply appeared since the

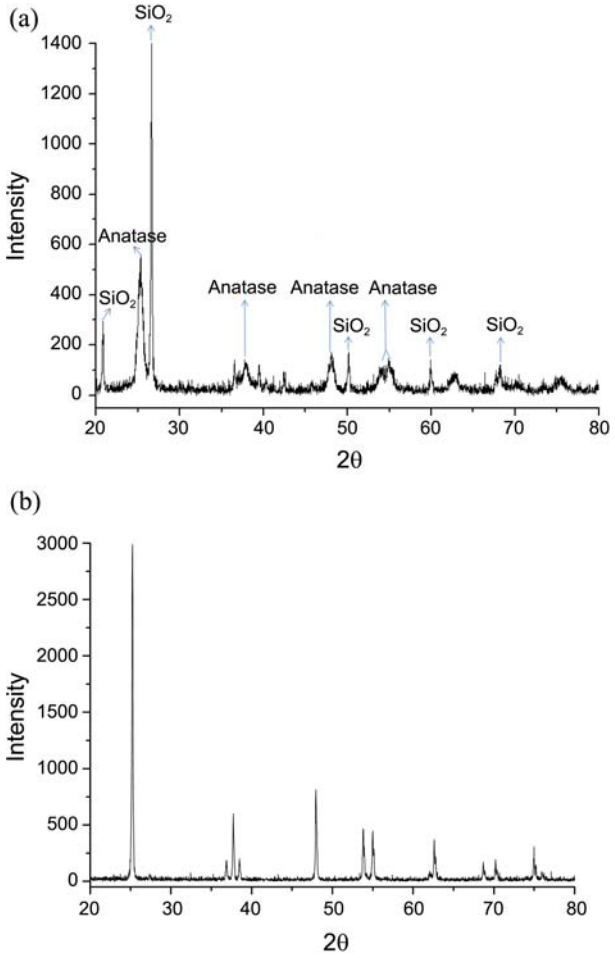

Figure 1. XRD pattern of (a) TiO_2-coated SiO_2 particles and (b) hollow TiO_2 after the elimination of SiO_2. All anatase peaks showed in Fig. 1(a) are disappeared.

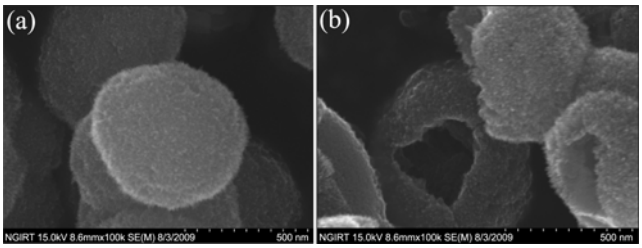

Figure 2. SEM images of (a) TiO_2-coated SiO_2 particles and (b) hollow TiO_2 after the elimination of SiO_2.

Table 1. XRF data of TiO_2 powders before and after the elimination of SiO_2

Element	Before elimination	After elimination
Ti	74.8%	99.8%
Si	24.0%	0.07%
Cl	1.0%	0%

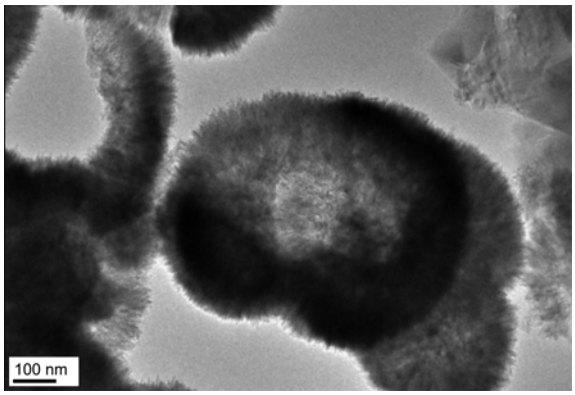

Figure 3. TEM image of hollow TiO_2.

major component in the particle is SiO_2 before the HF treatment. Only typical peaks of anatase phase are shown in the XRD result after the elimination of SiO_2 by treating the particles in the HF solution, as represented in Fig. 1(b). All reflections are assigned to anatase structure of TiO_2 and are indexed on the basis of JCPDS card No. 21-1272. Any peak corresponding to second phase is not detected, which means that all SiO_2 was eliminated.

SEM images of particles before and after the treatment with HF solution are shown in Figure 2(a) and Fig 2(b), respectively. TiO_2 is coated well onto the surface of SiO_2 and the size of the TiO_2-coated particles is about 300 nm diameter before the treatment with HF solution. Although not shown, the size of the TiO_2-coated particles depends on the temperature of the solution and the nucleation time of TiO_2 on the surface of a SiO_2 particle. After the treatment with HF solution, the core material (SiO_2) was eliminated and finally the TiO_2-coated spheres became hollow-structured TiO_2 particles. The wall of the hollow TiO_2 consists of hundreds of small TiO_2 particles whose sizes are within 20 nm. The thickness of the hollow wall is about 20-30 nm and the hollow is open through a hole whose diameter is about 150 nm. TEM image of the sample also demonstrates that the center of the particle is empty (see Fig. 3). The XRF analysis on the particles before and after the treatment with HF solution clearly shows that SiO_2 was completely eliminated after the treatment with HF solution (see Table 1). The SEM and TEM results are consistent with the XRF analysis data of TiO_2 hollow.

The UV spectroscopic data for the amount of dye absorbed by spherical and hollow TiO_2 samples are illustrated in Figure 4. The N719 dye shows typical absorbance peak at 230 nm in UV region. The peak area representing the amount of desorbed dye from spherical and hollow TiO_2 samples are 107 and 118, respectively. This means that hollow TiO_2 sample absorbs dye molecule more than 15% compared with spherical TiO_2 sample.

Application of the Synthesized Hollow TiO_2 Spheres to DSSCs. The performance of the DSSCs fabricated by using hollow TiO_2 powders was tested. Figure 5 shows the I-V characteristics of the cells made of hollow TiO_2 powders and that of a reference cell. The solar conversion efficiency of the reference cell (type A) which was prepared with 13 nm anatase as an electrode layer and 400 nm anatase as a scattering layer, was 9.29 %. The short-circuit photocurrent

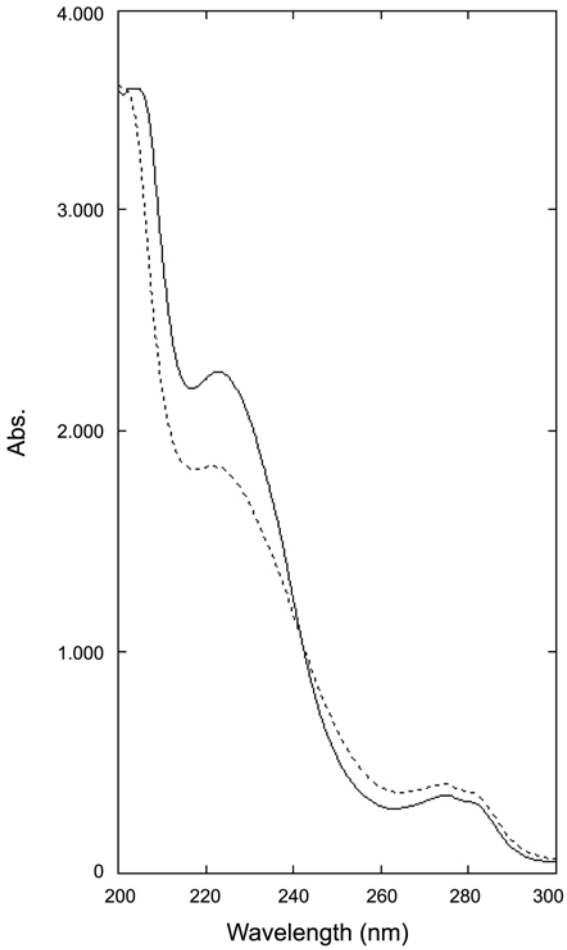

Figure 4. UV spectroscopy data for the amount of desorbed dye from hollow TiO_2 (solid line) and spherical TiO_2 (dotted line).

density (J_{sc}) and open circuit photovoltage (V_{oc}) were 17.8 mA/cm^2 and 0.73 V, respectively as shown in Figure 5(a). This result is consistent with the values obtained by other DSSCs research group when the same dye was used. The solar conversion efficiency of the cell was decreased to 3.58% when the hollow TiO_2 powders were used as an electrode layer material without any scattering layer (type D) as illustrated in Figure 5(d). The short-circuit photocurrent density (J_{sc}) and open circuit photovoltage (V_{oc}) were also decreased to 7.17 mA/cm^2 and 0.70 V, respectively (see Fig. 5(d)). The solar conversion efficiency of the cell (type C) which was fabricated with TiO_2 hollow spheres and 400 nm anatase spherical powders as an electrode layer and a scattering layer, respectively, was 4.59% as shown in Figure

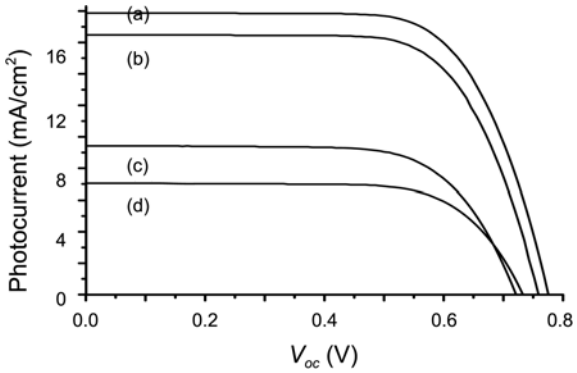

Figure 5. I-V characteristics of the different cells made of (a) 13 nm anatase and 400 nm anatase as electrode and scattering layer (type A), (b) 13 nm anatase and hollow TiO_2 as electrode and scattering layer (type B), (c) hollow TiO_2 and 400 nm anatase as electrode and scattering layer (type C), and (d) hollow TiO_2 only (type D).

5(c). Although the efficiency of this cell is higher than that of type D cell, it is still low compared with that of the reference cell. This means that large size (> 300 nm) anatase is not appropriate for the electrode material in a DSSC in spite of the shape of the powder. The conversion efficiency of the cell (type B) prepared with 13 nm anatase and hollow TiO_2 powders as electrode material layer and scattering layer, respectively, is shown in Figure 5(b). The solar conversion efficiency of type B cell is 8.45%, and the short-circuit photocurrent density (J_{sc}) and open circuit photovoltage (V_{oc}) were 16.5 mA/cm^2 and 0.72 V, respectively, which is similar to those of the reference cell. This result clearly shows that the size of the electrode material should be small to have the large surface area. The results of solar conversion efficiency, the short-circuit photocurrent density (J_{sc}) and open circuit photovoltage (V_{oc}) of each cell is summarized in Table 2. The photocatalytic efficiency of the hollow TiO_2 powders was slightly higher than that of P-25 sample.[20] It was proposed in the reference[20] that the hollow shape could contribute to absorb more light by using its empty space thereby increasing its photocatalytic efficiency. The DSSC result is contrary to the expectation that the solar conversion efficiency of the cell made of hollow-type TiO_2 spheres might be also increased by absorbing more dye molecules inside their empty cavities. It could be concluded, therefore, that submicron TiO_2 hollow spheres themselves cannot increase the solar efficiency of the DSSC as long as they were used as electrode material although they may absorb more amount of dye molecule.

Table 2. Characteristics of different solar cells

Cell type	V_{oc} (V)	J_{sc} (mA/cm^2)	η (%)
Reference Cell (13 nm TiO_2 + 400 nm TiO_2)	0.78	17.8	9.29
Hollow TiO_2 as an electrode layer without a scattering layer	0.74	7.17	3.58
Hollow TiO_2 + 400 nm TiO_2 as a scattering layer	0.72	9.49	4.59
13 nm TiO_2 + hollow TiO_2 as a scattering layer	0.76	16.5	8.45

Conclusions

TiO_2 hollow spheres were successfully fabricated by using an inorganic template. The thickness of the hollow wall is about 20-30 nm and the hollow is open through a hole whose diameter is about 150 nm. As the nucleation time of the mother solution ($TiOCl_2$) increased, the thickness of the hollow wall also increased. It is important, therefore, to control the time and the temperature of the crystallization process to obtain the appropriate TiO_2 hollow spheres. Obtained samples were applied for the fabrication of dye-sensitized solar cells. Since the size of the prepared TiO_2 hollow spheres is about 300-400 nm, this sample was tested in several ways; the sample was used as an electrode material (type C and type D) and was used as a scattering material (type B). When it was used as an electrode material, also two different type cells were prepared; first cell type was prepared by using TiO_2 hollow spheres as an electrode material without any scattering layer (type D), and the other cell type was prepared by adding a scattering layer which was made of 400 nm sized spherical anatase TiO_2 (type C). The results of solar conversion efficiencies, the short-circuit photocurrent densities (J_{sc}) and open circuit photovoltages (V_{oc}) of type C and type D cells were inferior to those of the type A reference cell and type B cell. The solar conversion efficiency of type B cell was similar to that of the reference cell. In conclusion, the solar conversion efficiency of the cell was low when TiO_2 hollow spheres were used as an electrode layer.

Acknowledgments. This work was supported by Wonkwang Research Fund of 2011. Authors thank to professor Ko at Korea university for invaluable discussions.

References

1. Kay, A.; Grätzel, M. *Sol. Energy Mater. Sol. Cells* **1996**, *44*, 99.
2. O'Regan, B.; Grätzel, M. *Nature* **1991**, *353*, 737.
3. Nazeeruddin, M. K.; Pechy, P.; Grätzel, M. *J. Am. Chem. Soc.* **2001**, *123*, 1613.
4. Nazeeruddin, M. K.; Kay, A.; Rodicio, I.; Grätzel, M. *J. Am. Chem. Soc*. **1993**, *115*, 6382.
5. Grätzel, M. *Inorg. Chem*. **2005**, *44*, 6841.
6. Adachi, M.; Murata, Y.; Takao, J.; Jiu, J. T.; Sakamoto, M.; Wang, F. M. *J. Am. Chem. Soc.* **2004**, *126*, 14943.
7. Jiu, J. T.; Isoda, S.; Wang, F. M.; Adachi, M. *J. Phys. Chem. B* **2006**, *110*, 2087.
8. Mor, G. K.; Shankar, K.; Paulose, M.; Varghese, O. K.; Grimes, C. A. *Nano Lett*. **2006**, *6*, 215.
9. Paulose, M.; Shankar, K.; Varghese, O. K.; Mor, G. K.; Hardin, B.; Grimes, C. A. *Nanotechnology* **2006**, *17*, 1446.
10. Mor, G. K.; Varghese, O. K.; Paulose, M.; Shankar, K.; Grimes, C. A. *Sol. Energy Mater. Sol. Cells* **2006**, *90*, 2011.
11. Park, N. K.; Schlichthrol, G.; van de Lagemaat, J.; Cheong, H. M.; Mascarenhas, A.; Frank, A. J. *J. Phys. Chem. B* **1999**, *103*, 3308.
12. Grunwald, R.; Trbutsch, H. *J. Phys. Chem. B* **1997**, *101*, 2564.
13. Ferber, J. Dissertation, University of Feiberg, 1999.
14. Ferber, J.; Luther, J. *Sol. Energy. Mater. Sol. Cells* **1998**, *54*, 265.
15. Rothenberger, G.; Comte, P.; Grätzel, M. *Sol. Energy. Mater. Sol. Cells* **1999**, *58*, 321.
16. Wang, Z. S.; Kawauchi, H.; Kashima, T.; Arakawa, H. *Coordinat. Chem. Rev.* **2004**, *248*, 1381.
17. Hore, S.; Vetter, C.; Kern, R.; Smit, H.; Hinsch, A. *Sol. Energy. Mater. Sol. Cells* **2006**, *90*, 1176.
18. Choi, H.; Baik, C.; Kang, S. O.; Ko, J.; Kang, M.-S.; Nazeeruddin, Md. K.; Grätzel, M. *Angew. Chem. Int. Ed*. **2008**, *47*, 327.
19. Kim, C.; Choi, H.; Kim, S. H.; Baik, C.; Song, K. H.; Kang, M.-S.; Kang, S. O.; Ko, J. *J. Org. Chem*. **2008**, *73*, 7072.
20. Cho, H. J.; Hwang, P.-G.; Jung, D. *J. Phys. Chem. Solids* submitted.